SPATIAL PATTERNS OF THREADLIKE ELEMENTS IN THE AXOPLASM OF THE GIANT NERVE FIBER OF THE SQUID (*LOLIGO PEALII* L.) AS DISCLOSED BY DIFFERENTIAL INTERFERENCE MICROSCOPY AND BY ELECTRON MICROSCOPY

J. METUZALS and C. S. IZZARD

From the Department of Histology and Embryology, Faculty of Medicine, University of Ottawa Ottawa, Canada; the Department of Biological Sciences, State University of New York, Albany New York 12203; and the Marine Biological Laboratory, Woods Hole, Massachusetts 02543. Dr. Metuzals' present address is the Institute of Neurobiology, Faculty of Medicine, University of Göteborg, Göteborg, Sweden

ABSTRACT

The giant nerve fiber of the squid (*Loligo pealii* L.) has been investigated *in situ*, and in fresh and fixed preparations, by differential interference microscopy and electron microscopy. A continuous, three-dimensional network, composed of threadlike elements, was disclosed in the axoplasm. The threadlike elements in the axoplasm are twisted as a whole into a steep, right-handed helix. In a peripheral ectoplasmic region, the elements are more parallel to one another and more densely packed than in a central endoplasmic core. The threadlike elements can be resolved into a hierarchy of decreasing order of size. Successive levels of the hierarchy are formed by the association of smaller elements into larger ones. The following levels in the hierarchy of network elements have been distinguished: 1–3-μ-wide threads, 0.1–0.35-μ-wide strands, and 70–250-A-wide unit-filament strands. The differential interference microscope selects, from the network, threads oriented at a specific angle to the long axis of the axon. The specific angle depends upon the orientation of the long axis of the axon relative to the direction of shear. It is postulated that the network configuration is expressed in the solid-state properties of the axoplasm essential for the normal functioning of the nerve fiber.

INTRODUCTION

There are numerous experimental observations which indicate that the axoplasm of the fresh giant nerve fiber of the squid is normally in a gelled state and behaves like a solid (Hodgkin and Huxley, 1945; Hodgkin and Katz, 1949; Chambers and Kao, 1952; Baker, Hodgkin, and Shaw, 1962). Furthermore, several observations suggest that the structural integrity of the axoplasm, expressed in its gelled state, is essential for the normal functioning of the fiber. Injured regions of the axon commonly become liquefied, lose their excitability, and their contents flow out when the axon is cut. Microinjection of calcium liquefies the axoplasm and tends to block conduction (Hodgkin and Keynes, 1956).

Generally, it is accepted that the ~100-A-wide

neurofilaments, extending as independent longitudinal units, represent the main structural framework of the axoplasm in spite of the fact that the behavior of the fresh axoplasm is difficult to reconcile with a structural array having only one-dimensional order. For example, as was first described by Bear, Schmitt, and Young (1937 *a*), a jelly-like and apparently solid cylinder of axoplasm is obtained when the contents of a fresh giant nerve fiber of the squid are extruded from the sheath.

We have observed in the axoplasm of the sqiud giant nerve fiber a specific three-dimensional network of threadlike elements. This three-dimensional structure conforms well with the gel-state properties of fresh axoplasm. The complex network pattern was discerned by integrating observations of fresh giant nerve fibers made with the differential interference microscope with observations obtained by electron microscopy of fixed material.

The current development of the differential interference microscope (Nomarski, 1955; Françon, 1961; Bajer and Allen, 1966 *a* and *b*; and for more extensive reviews Padawer, 1968; Allen, David, and Nomarski, 1969), provides a powerful tool for investigating the structure of the giant nerve fiber of the squid under fresh and living conditions. Through the use of the differential interference microscope, phase objects are revealed as a high-contrast image in which the resolution limit of the light microscope is closely approached. Optical sectioning of thick structures can be effected with minimal interference from objects lying above or below the plane of focus. Therefore, with this instrument, detailed and close correlations can be sought between structural patterns existing in the living fiber and those resolved by electron microscopy. If found, these correlations provide a sound basis for interpreting the patterns of the fixed material in terms of the living state. Furthermore, the possibility of surveying large areas with the differential interference microscope allows spatial patterns to be discovered which otherwise would only be hinted at by electron microscopy.

The axons of cephalopod giant nerve fibers were investigated with the light microscope by Young (1937). Bear, Schmitt, and Young (1937 *b*) have investigated in polarized light the ultrastructure of the axoplasm in fresh giant fibers of the squid. Electron microscopy of thin sections of fixed giant fibers was carried out by Schmitt and Geren (1950), Geren and Schmitt (1954), Villegas and Villegas (1960 *a* and *b*), and Baker, Hodgkin, and Shaw (1962).

In the following, the results of an investigation of the squid giant nerve fiber, obtained by the methodological approach outlined above, will be reported. A preliminary account has appeared elsewhere (Metuzals, Izzard, and Gospodnetić, 1968).

METHODS

Materials

The experiments were carried out with living squid (*Loligo pealii* L.) obtained at the Marine Biological Laboratory, Woods Hole, Mass. during the summers of 1966, 1967, and 1968. The animals used for fresh or fixed preparations had spent no more than a few hours in laboratory tanks containing running seawater. For each of the following preparative methods, the animals were decapitated and the mantle cavity was opened. Dissection of one of the dorsal giant nerve fibers was performed under running seawater on a dissecting table illuminated from below through a glass window.

Light Microscopy

Fresh Giant Nerve Fibers

Zeiss/Nomarski differential interference contrast equipment for transmitted, or reflected, light was fitted to a Zeiss (Carl Zeiss, Inc., New York) Photomicroscope I stand. The light source was either an Osram HBO-200 mercury-vapor arc used in conjunction with a green narrow-band interference filter (546 mμ), or a low-voltage (12 v, 5A) tungsten lamp used with a wide-band interference filter (approximately 546 mμ).

TRANSMITTED LIGHT: A 5-cm portion of the giant nerve fiber was dissected free of connective tissue and removed from the mantle wall, attached at one end to the stellate ganglion, and ligated at the other end. The *fresh* preparation was mounted under a supported coverslip in seawater on a large No. 1½ coverslip. For reducing the thickness of the preparation, only the nerve fiber was covered. The ganglion remained outside the coverslip and was bathed at intervals during the period of observation with fresh seawater. Such preparations routinely remained in good condition for 1½ hr, after which large fluid-filled vesicles developed in the superficial axoplasm of some preparations. Although the threadlike elements appeared to be unaffected, all preparations were discarded after an interval of 1½ hr.

The nerve fiber was examined with Planachromat 16/0.32, Achromat 40/0.85 oil immersion, and Planachromat 100/1.25 oil immersion objectives.

Operational extinction factors (see Allen, David, and Nomarski, 1969) ranged from 150 for the 16/0.32 objective to 250 for the 100/1.25 oil immersion objective. (The extinction factor for the differential interference microscope, as for any other polarizing microscope, provides a measure of the ability of the system to generate contrast detectable above the background noise that results from stray light in the system.) A precentered polarizing stage was used for determining the angular orientation of the nerve fiber relative to the direction of the shear. The optical train (objectives, mounted in single centering objective-changers, and condenser) was aligned to the fixed center of rotation of the stage.

REFLECTED LIGHT: The giant nerve fiber was examined *in situ* with the Zeiss/Nomarski reflected light, differential interference contrast equipment (Zeiss operating instructions G-41-655-e) fitted with 8/0.2 *Pol* and 16/0.35 *Pol* epiplan objectives.

On the dissecting table under running seawater, a portion (1 cm in length) of the nerve fiber was cleared of skin and connective tissue, and a fragment of coverslip, coated first with aluminum and then with a $\lambda/2$ layer of SiO, was inserted between the nerve fiber and mantle as a reflecting surface. The whole preparation was pinned flat in a dish, covered with seawater, and placed on the microscope stage for examination.

Fixed Giant Nerve Fibers

Giant nerve fibers were fixed in glutaraldehyde and osmium tetroxide for electron microscopy and embedded in Vestopal W as outlined below. Thick (2-μ) longitudinal sections, either unstained or lightly stained with 1% methylene blue in 1% borax (after Richardson, Jarett, and Finke, 1960), and mounted in neutral balsam, were examined by differential interference microscopy. With stained sections, phase contrast and amplitude contrast were routinely used (see Padawer, 1968, and Allen, David, and Nomarski, 1969). Operationally, the instrument is set at extinction, bias compensation is introduced so as to produce maximal contrast due to phase differences in the object, and finally, by rotating the polarizer a few degrees, amplitude contrast is generated for further increasing the contrast of the optical image. Extinction factors up to 400 were obtained for the 100/1.25 objective with these preparations. Unstained sections were also examined by Reichert anoptral phase-contrast (100/1.25 oil immersion) in the Reichert Zetopan microscope (Reichert, Austria; American Optical Corp., Buffalo, N.Y. 14215)

Electron Microscopy

Four main fixation procedures have been used: (*1*) glutaraldehyde and osmium tetroxide; (*2*) osmium tetroxide; (*3*) uranyl acetate solution followed by osmium tetroxide; (*4*) sodium phosphotungstate followed by glutaraldehyde and osmium tetroxide. Dehydration, embedding, sectioning, and staining have been carried out in the usual manner. Full details of these procedures are given in another paper (Metuzals, 1969).

RESULTS

The main result of this investigation is the demonstration of a continuous, three-dimensional network extending in a regular pattern throughout the axoplasm of the squid giant nerve fiber. The network is composed of *threadlike elements* which can be resolved into a hierarchy of decreasing order of size. The smallest element is resolved only in high magnification electron micrographs and is dealt with in another paper (Metuzals, 1969). Successive levels of the hierarchy are formed by associations of the smallest elements into larger units. At each hierarchic level the elements branch, interconnect, and intercoil to form a network, and in so doing build up the next hierarchic level. Through the analysis of the axoplasm at successively higher levels of resolution, it became evident that the morphological entities, delineated and analyzed in the present paper, are determined (*1*) by the resolving power of the instrument used and (*2*) by the statistically uneven distribution and

FIGURES 1 and 2 The figures represent different levels of optical sectioning through the same area of a fresh giant nerve fiber of the squid. Differential interference 16/0.32. The orientation of the long axis of the fiber is identical in both figures and is approximately vertical. Arrow in either upper corner indicates direction of shear. Fig. 1 illustrates a section through the surface region of the axon, whereas Fig. 2 illustrates a section passing through the center of the fiber. The structural elements of the sheath (*S*) and of the axoplasm can be clearly distinguished. The axoplasm consists of parallel threadlike elements about 1.5–3.0 μ in diameter. Note the different orientation of the threadlike elements in the two figures. The vertical lines in Fig. 2 indicate the approximate boundaries between the ecto- and endoplasm (*EC, EN*) of the axon. The threadlike elements are more prominent in the ectoplasm than in the endoplasm. × 353.

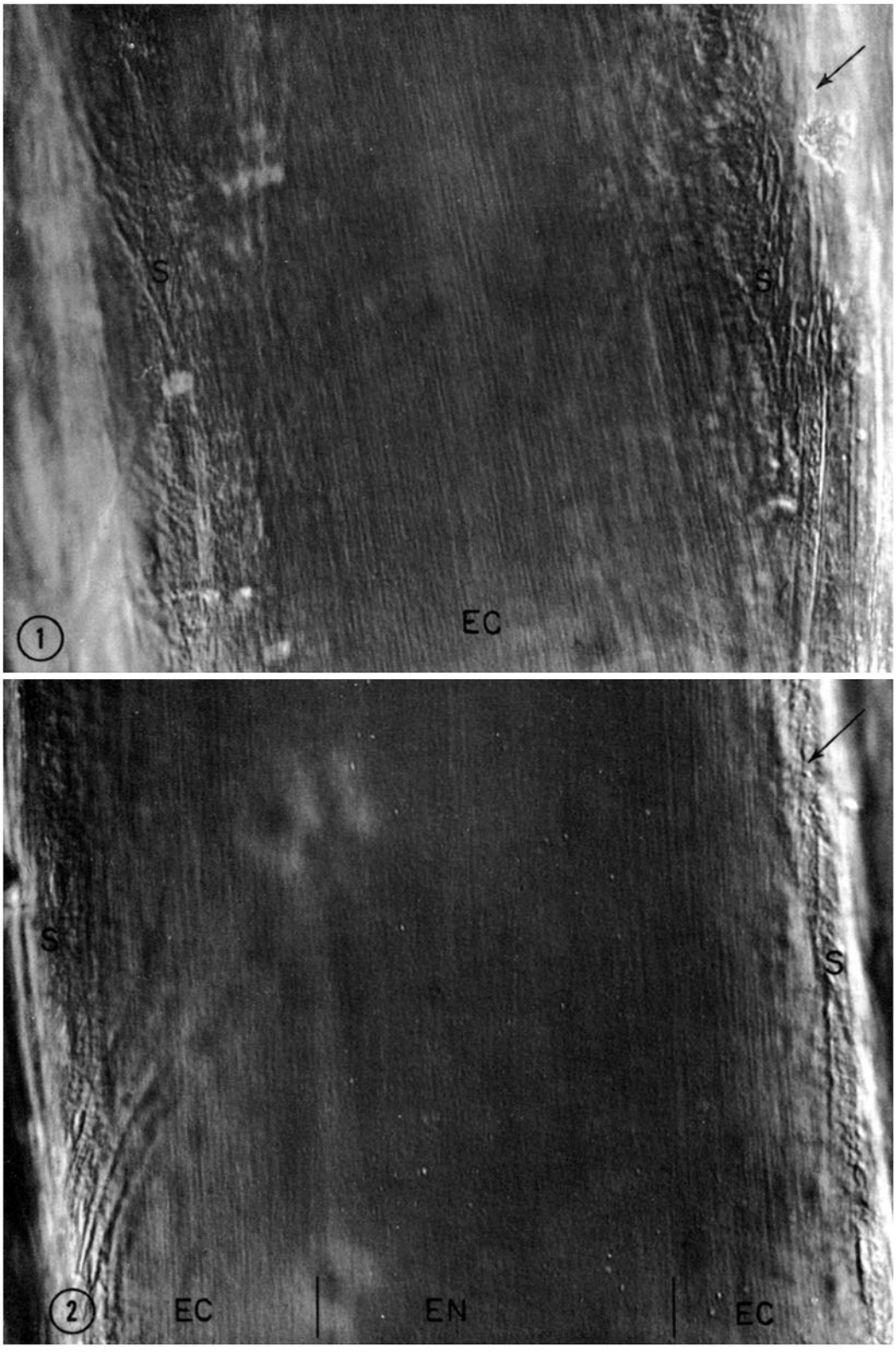
S
S
EC
1
S
S
EC
EN
EC
2

orientation of entities beyond the particular level of resolution.

An important aspect of the results is the close correlation of the appearance of the network elements revealed at various levels of resolution in the living fibers with the appearance of these elements in electron micrographs of fixed fibers. In many respects, the organization of the axoplasm of the squid giant nerve fiber emphasizes a central problem of morphology—that is, the problem of delineation and meaning of structural units in a living system and the relationship of such a delineation to the resolution of the instrument used.

Light Microscopy

General Features of the Living Giant Nerve Fiber

The sheath surrounding the axoplasm consists of Schwann cells, connective tissue wrappings, and small blood vessels. All these structures can be identified readily in living fibers with the differential interference microscope and can be distinguished with certainty from the axoplasmic elements. Since out-of-focus structures do not contribute significantly to the contrast image of the differential interference microscope, the presence of the sheath in the fresh preparations does not hinder the optical sectioning of the axoplasm.

At the light microscopic level, the main structural differentiations of the axoplasm are distinct, threadlike elements and oval, or round, bodies of varying size (Figs. 1, 3, and 8). The dimensions of the *threads* differ in 16/0.32 and 40/0.85 differential interference micrographs. Respectively, the threads measure 1.5–3.0 μ (Figs. 1 and 2) and 0.4–0.8 μ (Figs. 8 and 15) in diameter. Clearly the larger threads have been resolved into finer threads. Groupings of threads in Fig. 8 (indicated by opposed paired arrows) measure 1.5–2.5 μ in width and are the structural counterpart of the threads in the 16/0.32 differential interference micrographs (Figs. 1, 2, and 6). Elongate granules, 0.4–0.8 μ wide and oriented parallel to the threads in Figs. 8 and 19, are absent in the lower resolution micrographs and have been "optically absorbed" into the larger threadlike elements.

Generally, a peripheral *ectoplasmic* and a central *endoplasmic* region can be distinguished in the axoplasm by differences in the orientation, arrangement, and packing of the threadlike elements. At lower magnification, the ectoplasmic region exhibits a denser, predominantly parallel, packing of straight threads (Figs. 1, 2, and 6). In contrast, the threads often show a looser reticular array in the endoplasm (Figs. 2 and 6). Without exception, the threads in the ectoplasm are oriented at an angle of 5–20° to the longitudinal axis of the nerve fiber (Fig. 1). In longitudinal optical sections of the upper ectoplasm, the orientation of this angle relative to the axis of the fiber is opposite to that in sections of the lower ectoplasm, indicating that the threads are wound helically along the fiber. In a number of preparations, it was determined that the threads are wound in a right-handed helix. The pitch of the helix of the threadlike elements in the fiber of Figs. 1 and 2 was calculated to be approximately 5 mm. The threads in fixed axons are similarly oriented at an angle to the long axis of the fiber.

Occasionally, the threads of the endoplasm are grouped in bundles, each having a different orientation relative to the fiber axis. Such bundles may intercoil to produce a large scale ropelike pattern in the axoplasm (Figs. 3 and 4). In some portions of the endoplasm, sinusoidal threads are in register across the width of the fiber, resulting in the over-all appearance of large-scale cross-banding. Within each successive cross-band, the thread orientation, therefore, reverses relative to the long axis of the nerve fiber.

All the structural features outlined above were confirmed in the *in situ* nerve fiber examined by reflected light, differential interference microscopy.

Fiber Orientation in the Axoplasm Analyzed by Rotation Experiments

RATIONALE FOR ROTATION EXPERIMENTS: In the differential interference microscope, the contrast image results from the interference of two, laterally misaligned, replicate images produced by the optical shearing effect of the beam splitter or upper Wollaston prism. Since the optical shearing is very small the system has a directionality in its interfering wave fronts, and contrast is generated from gradients of optical path difference lying parallel to the preferred direction of shear. The direction of shear is fixed in the microscope. Therefore, objects lacking spherical symmetry must be rotated in order to bring all optical gradients successively parallel to the direction of shear and thus reveal the different features of interest (Bajer and Allen, 1966 *a*;

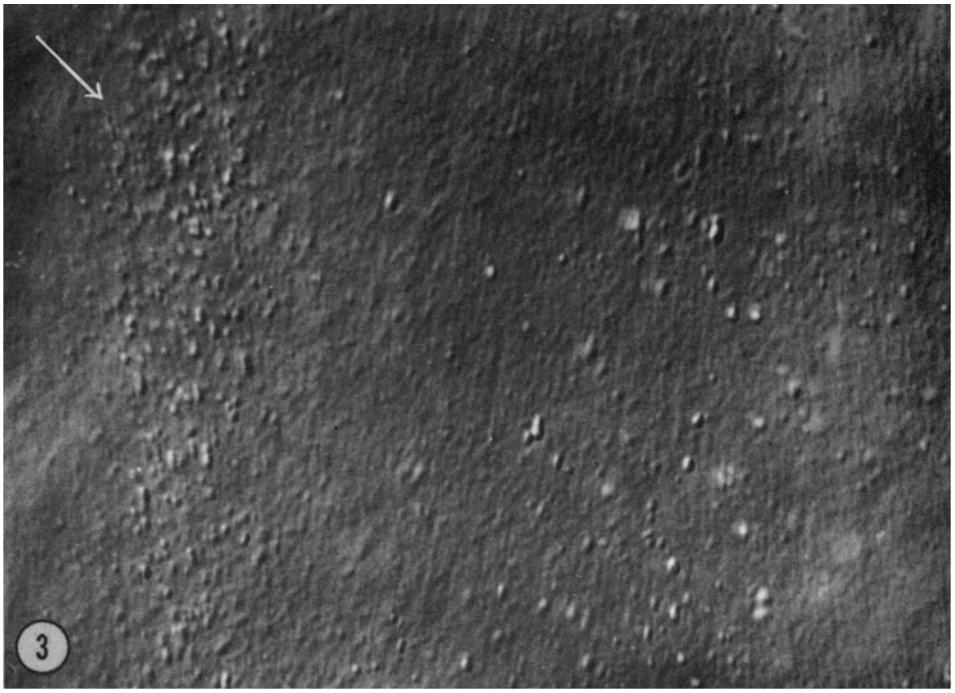

FIGURES 3 and 4 Optical sections through the axo-plasm of a fresh giant nerve fiber of the squid. Differential interference 16/0.32. Long axis of the fiber vertical.

FIGURE 3 Groups of axoplasmic threads oriented at different angles to the fiber axis. × 448.

FIGURE 4 Large-scale ropelike pattern in the axo-plasm produced by intercoiling bundles of threadlike elements. × 224.

Padawer, 1968; Allen, David, and Nomarski, 1969). The direction of shear is indicated in each of the figures by a heavy arrow in one of the upper corners of each figure.

In a linear structure, such as a fiber, maximum contrast is generated when the long axis of the structure is oriented at 90°, or orthogonal, to the direction of shear (see Figs. 5, 6). When the long axis is rotated from this position, the gradient of optical path difference across the fiber in the direction of shear decreases until it reaches zero when the long axis is parallel to the direction of shear. From purely geometrical considerations, the optical gradient in the direction of shear, and hence the contrast generated, decrease as a function of the cosine of the angle of rotation from the orthogonal position. Being a cosine function, contrast does not fall off rapidly, and, after 30, 45, and 60° rotation, contrast is reduced by 13, 29, and 50%, respectively (see Padawer, 1968, and Allen, David, and Nomarski, 1969, for further discussion).

If fibers in a system are oriented up to +45 or −45° about a mean direction, all the fibers should be adequately contrasted when the mean fiber direction is arranged orthogonal to the direction of shear. However, if the fibers that deviate from the mean direction are fewer in number and/or finer in structure than the predominant, more heavily contrasted, orthogonal fibers, the latter may partially obscure or detract from the former. Thus, for investigating the full range of angular orientation of fibrous elements in the axoplasm, the mean fiber direction was arranged parallel to the direction of shear. Then the specimen was rotated through 90° at 5 or 10° intervals during which contrast was generated initially by fibers showing the greatest deviation from the mean direction, and successively by fibers more nearly parallel to the mean direction. The specimen was photographed at each interval, and the focus was not changed throughout each series. With fresh preparations, it was necessary to adjust bias compensation at each interval, but with stained and unstained sections, amplitude matching and/or bias compensation were not altered.

ECTOPLASM: The extended threadlike elements, characteristic of the ectoplasm in low-magnification light micrographs of fresh (Figs. 1, 2, and 6) or sectioned material, do not deviate significantly from a parallel orientation.

The same is essentially true in longitudinal optical sections of fresh material at a somewhat higher magnification (40/0.85 oil immersion). When examined in detail at this magnification (Fig. 8), a few threads deviate from the mean orientation in each step of the rotation series. Relative to a fixed axis in the axon, which can be defined by reference to granules, the total angular spread of such threads measured from the complete rotation series was 8°. These angular deviations are not resolved with the 16/0.32 differential interference equipment.

Further analysis at higher resolution was limited by light scatter which reduces excessively the contrast attainable in the thick, fresh preparations of the giant nerve fiber. For this reason, the fresh ectoplasm was examined only in the orthogonal position with the 100/1.25 differential interference equipment.

A small area of a longitudinal optical section, taken 14 μ below the surface of the fresh axon, is illustrated in Fig. 9. Well contrasted, elongate granules, 0.5 μ in width and 1–3 μ in length, lie

FIGURES 5 and 6 Longitudinal optical sections through the center of the fresh giant nerve fiber of the squid. Differential interference 16/0.32. Each section is at the same level in the axoplasm. Approximately half of the width of the axon is included in each figure.

FIGURE 5 Long axis of axon is parallel to the direction of shear. Note the distinctive cross-lattice pattern in the endoplasm (*EN*), oriented symmetrically about the direction of shear and the long axis. Each component of the cross-lattice consists of fine threadlike elements (arrows). *EC*, ectoplasm; *S*, sheath.

FIGURE 6 Approximately the same area of the optical section in Fig. 5, but rotated 90° so that the long axis is orthogonal to the direction of shear. Note the threadlike elements in the axoplasm, and the different form of the elements in the ectoplasm (*EC*) and in the endoplasm (*EN*). Arrows indicate 1.5-μ threads interwoven in ropelike structures. *S*, sheath. Both figures, × 480.

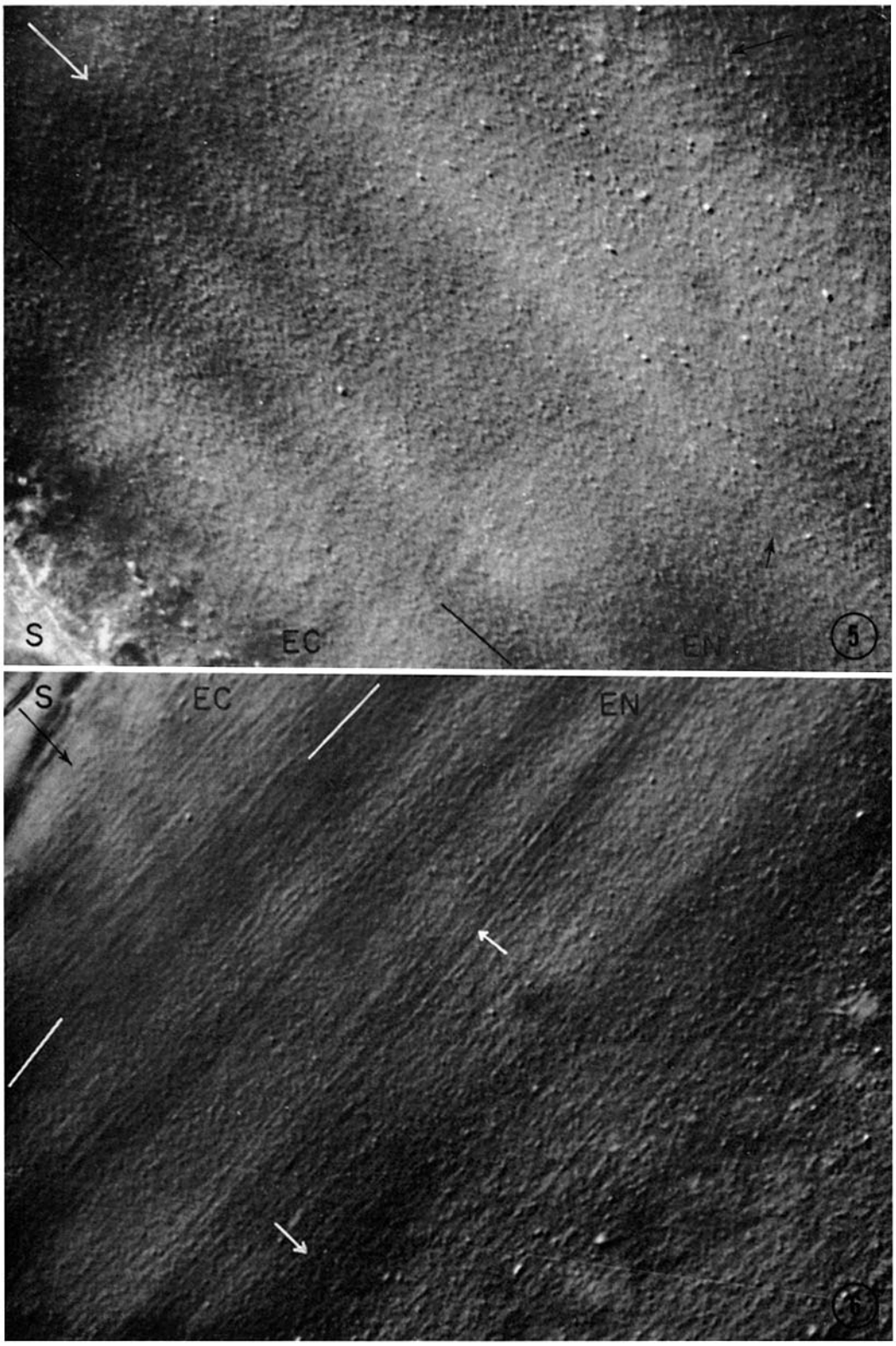
S
EC
EN
5
S
EC
EN
6

with their long axes more or less parallel to one another and to the long axis of the axon. Thin, low-contrast *strands* extend up to 10 μ in the optical section. The individual course of each strand is gently curved in the optical section, indicating an over-all sinuous course. 1.5–2.5-μ-wide groupings of two to four strands can be delineated over much of the figure and are indicated by opposed, paired arrows. The groupings are not discrete but bifurcate, and hence approach or join other groupings in the optical section. They represent the threads in the low-resolution micrographs in which such bifurcations and junctions are not clearly resolved.

Measurement of the diameter of the strands is difficult in the "shadow-cast" image. Isolated strands, i.e. strands contrasted against a uniform-intensity background, measure 0.35 μ in diameter if the strand is considered to be delineated on one side by a bright peak and on the other by a dark peak. In close groupings, a clearly defined space cannot be readily distinguished between strands. However, measured by reference to the repeat period of the brightest points in the shadow-cast image, the parallel strands show a minimum center-to-center spacing of 0.45 μ. This repeat period includes one strand diameter and one separation space, and thus, from these measurements, the strand diameter should be close to the 0.35-μ diameter given above.

Since rotation experiments were not possible with fresh material under the 100/1.25 differential interference equipment, 2-μ Vestopal sections were used for checking whether or not, at high resolution, strands are oriented in directions other than those given above. Identical results were obtained for the ectoplasm from medial, and superficial longitudinal sections of the axon, demonstrating that the angular spread of the fibers is symmetrical about the mean fiber orientation. Selected steps from one rotation series are illustrated in Figs. 10–13. In each figure, the same area of a longitudinal section is depicted, and the long axis of the axon is oriented vertically on the page, so as to facilitate comparison of fiber orientation. Hence, the direction of shear rotates relative to the long axis in an anticlockwise direction from a vertical position in Fig. 10 to a horizontal position in Fig. 13.

The four steps in the rotation are distinctive: in the parallel position granular detail predominates (Fig. 10); after 30 and 50° rotation, fine strands and granules are present (Figs. 11 and 12); and in the orthogonal position, a rather coarse, fibrous detail is present (Fig. 13). Comparison of Figs. 11, 12, and 13 shows that the groupings of strands and associated granules resolved after 30° rotation have "fused optically" to produce the coarse elements in Fig. 13. The effect is dramatic when observed in the microscope, and consistently a 30–40° orientation of the predominant axis of the strands relative to the direction of shear can be selected to give maximum resolution of fine detail. At this orientation, the smallest center-to-center distance of parallel strands measured 0.33 μ (Fig. 11, arrow *1*), whereas in the orthogonal position the smallest center-to-center distance measured 0.45 μ (Fig. 13, small arrow). The difference in resolving ability does not arise from a failure to readjust bias compensation to contrast selectively the finest elements of the axoplasm at each step in the rotation. An exactly similar effect is observed with the 16/0.32 and 40/0.85 differential interference equipment in fresh and sectioned material. This feature of differential interference microscopy has not been commented on previously, and at the present it is not possible to provide an adequate explanation of the phenomenon in terms of the optical properties of the differential interference

FIGURES 7 and 8 Longitudinal optical sections through the ectoplasm of the axon of a fresh giant nerve fiber. Differential interference 40/0.85 oil. Both sections cover the same area of the fiber and lie at almost identical focal planes.

FIGURE 7 The predominant axis of the threadlike elements is oriented parallel to the direction of shear. The threadlike elements are not contrasted. Note the cross-lattice pattern, delineated by the orientation of many of the elongate granules, and partly by fine strands (arrows). *N*, Schwann cell nucleus; *S*, sheath. × 1,200.

FIGURE 8 The preparation in Fig. 7 rotated 40°. Note the contrasted threadlike elements running approximately parallel to one another. Individual threads deviate from the mean orientation (single arrows). Close groupings of threadlike elements are indicated by opposed, paired arrows. *N*, Schwann cell nucleus; *S*, sheath. × 1,200.

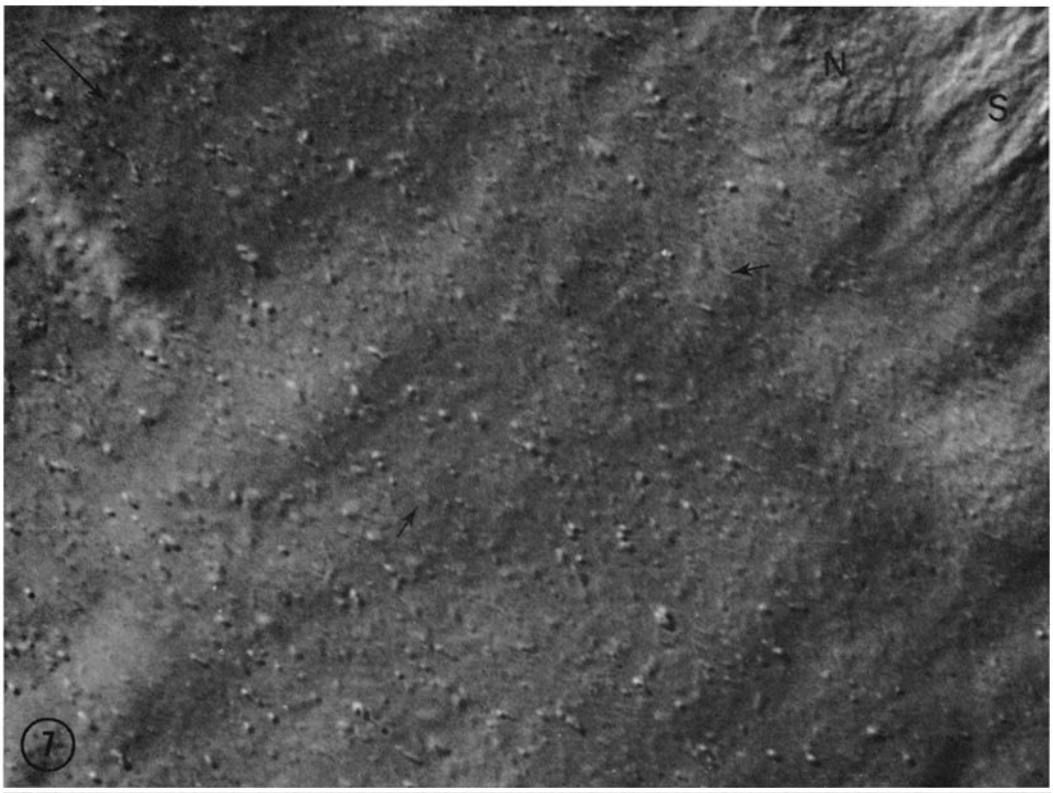
N
S
7

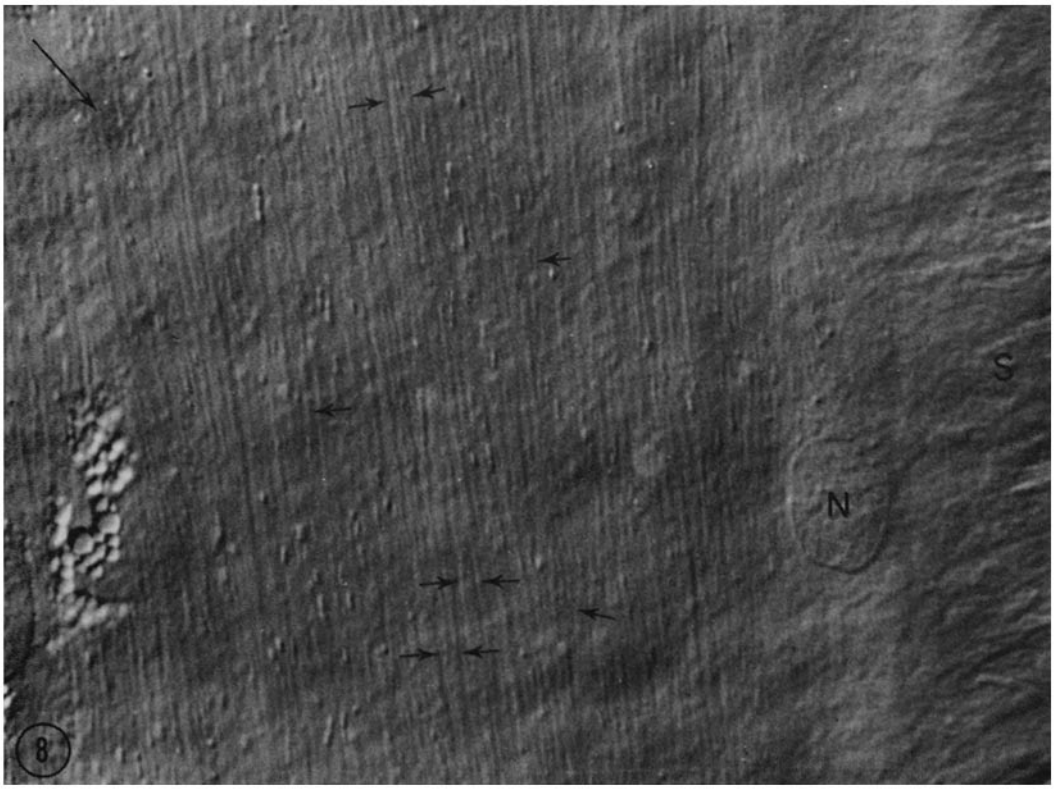
S
N
8

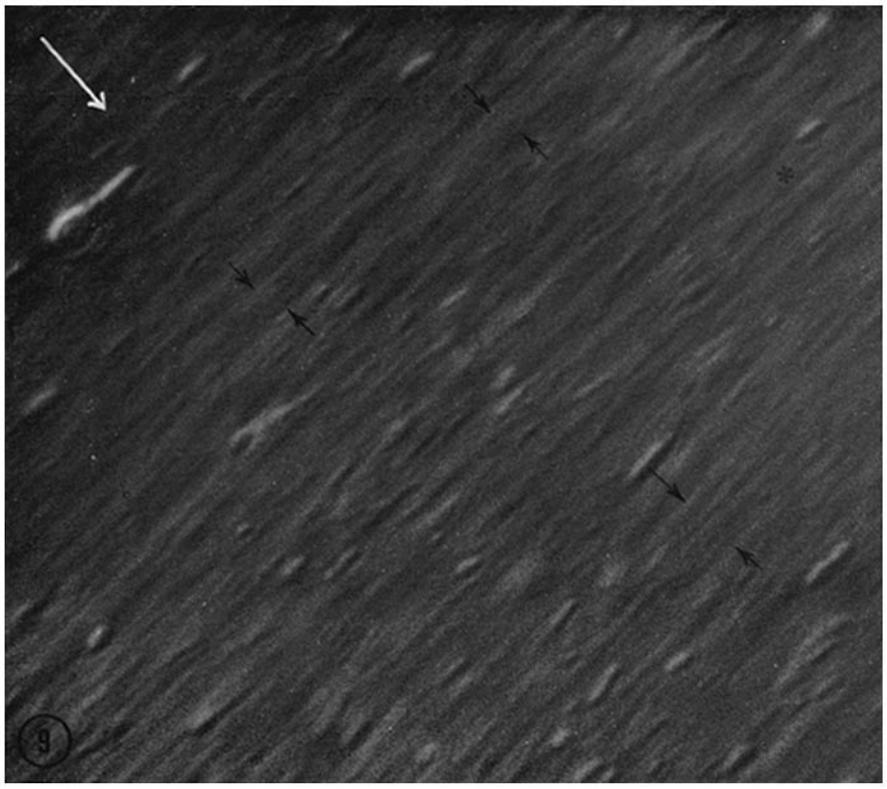

FIGURE 9 Optical section of the ectoplasm taken 14 μ below the surface of a fresh axon of the giant nerve fiber of the squid. Differential interference 100/1.25. The predominant axis of the threadlike elements is oriented at 90° to the direction of shear. Fine linear strands can be distinguished over much of the figure. In areas, the strands are arranged into close groupings (paired, opposed arrows). The groupings are not discrete but branch and join with one another (see region indicated by the asterisk). × 3,000.

microscope. However, the phenomenon influences and is of practical significance in the analysis of fiber orientation in the axoplasm.

The strands contrasted at 30 and 50° rotation (Figs. 11 and 12), and the unresolved groups of strands contrasted at 90° rotation (Fig. 13), run more or less parallel to the long axis of the axon. As in the fresh material, individual strands follow a slightly sinuous course passing from one close grouping to another. The fine granular detail of Fig. 10 is oriented in linear arrays that indicate the course of the longitudinal strands in Fig. 11. However, at either side of Fig. 10, weakly contrasted, parallel strands run obliquely from NE to SW at an angle of nearly 20° to the longitudinal axis. These oblique strands first gradually increase in contrast during the rotation and finally are not resolved in the optical image when they make an angle of 50° or more to the direction of shear (Fig. 11). Short segments of strands run obliquely in the opposite direction in the lower right-hand corner of Fig. 10. During rotation, these strands disappear from the image as they pass through the position parallel to the direction of shear. After 50° rotation of the preparation, similarly oriented strands appear again at the lower right-hand corner of Fig. 12. The strands now make an angle of 35° to the direction of shear, and thus generate adequate contrast and lie at the preferred angle for the resolution of fine detail. The limited number of short strands, oriented at angles of 15–20° on either side of the longitudinal axis, does not represent an independent array of strands. On the contrary, the strands represent short lengths of the longitudinal arrays that deviate from the predominant orientation to cross from one close grouping

to another. Such continuity of differently oriented strands can be followed from Fig. 11 (arrow *1*) to Fig. 12 (arrows *1* and *2*). The rotation of the sectioned axon reveals essentially the same structural configuration that was deduced for the ectoplasm from the examination of living tissue in the orthogonal position. The sole addition to the configuration is a limited number of strands deviating to a greater extent from the predominant orientation.

In fresh material, evidence for a similar deviation of the strands has been obtained with 40/0.85 differential interference equipment. When the predominant threads are oriented parallel to the direction of shear (Fig. 7), a faint "cross-lattice" pattern can be detected. The two components of the lattice are arranged symmetrically about the direction of shear and make an angle of approximately 40° to one another. The lattice can be detected by the orientation of the long axes of many of the granules and, in two areas, by very low contrast, fine linear strands (arrows in Fig. 7). The orientation of the granules is considered to express underlying fibrous orientations.

ENDOPLASM: The individual threadlike elements of the endoplasm, resolved at low magnification, are shorter in length, more irregular in outline, and less parallel to one another than those in the ectoplasm. This is true within each of the different large-scale configurations exhibited by the endoplasm. In fresh (Fig. 5) and fixed material, the predominant threadlike elements are not contrasted when the longitudinal axis of the axon is oriented parallel to the direction of shear. However, a prominent cross-lattice pattern is present in both fresh and fixed material. The two components of the lattice consist predominantly of short (6–10-μ), but also long (20-μ), threads measuring 1.0–1.5 μ in diameter. The angle between the two components of the lattice ranges from 45 to 55° in various preparations and is divided more or less equally on either side of the direction of shear. Similarly, in higher resolution micrographs (40/0.85 differential interference equipment) a low-contrast cross-lattice pattern in fresh (Fig. 14), and a pronounced cross-lattice pattern in sectioned (Fig. 16), material are present when the longitudinal axis of the axon is oriented parallel to the direction of shear. The lattice again consists of threadlike elements, but at this higher level of resolution, the diameter of the threads is now 0.5–0.8 μ. Relative to the direction of shear, the threads in each component of the cross-lattice lie approximately at the preferred angle for the resolution of fine detail and also at an angle that generates 50% of the maximum contrast available in the orthogonal position.

On rotating the fresh or fixed preparation from the parallel position, the component of the cross-lattice towards which the longitudinal axis rotates remains more or less fixed relative to the direction of shear at an angle of approximately 30°. Therefore, the angle between this component and the longitudinal axis decreases until the two are parallel after 30–40° rotation (Figs. 2 and 15—respectively, 16/0.32 and 40/0.85 micrographs). During the rotation the instrument has selected, at successive angles between the initial cross-lattice and the longitudinal axis, threads spaced at or near the resolution limit of the particular objective used. The threads contrasted in this way become more prominent as they are selected more nearly parallel to the long axis of the axon. The other component of the initial lattice, away from which the longitudinal axis rotates, fades quickly during the first few degrees of rotation. Therefore, the threads resolved with 16/0.32 and 40/0.85 differential interference equipment are not oriented at angles greater than 30° from the longitudinal axis of the axon. The same sequence of events occurs if the preparation is rotated in either direction from the parallel position. Hence, the conclusion can be made that the widest, angular deviation of the threads from the longitudinal axis is defined by the total spread of the initial cross-lattice and that threads lie at all intermediate angles between the cross-lattice.

With continued rotation, the threads parallel to the long axis at the 30° rotation step retain their orientation relative to the long axis and, rotating with the axon, progressively break down into the coarse, shorter elements seen in Fig. 6 in the orthogonal position. Comparison should be made at this point between the appearances of the threads in the fresh endoplasm and ectoplasm in Fig. 6: the shorter extent and more irregular form of those in the endoplasm is immediately apparent. Similarly, the difference in linear extent is apparent when the longitudinal threads are most clearly resolved at an orientation of 30–40° to the direction of shear (compare Figs. 8 and 15). This difference, and the pronounced angular spread of the threads in the endoplasm as compared with the ectoplasm, are interpreted to mean that in the endoplasm no thread is discrete for any great

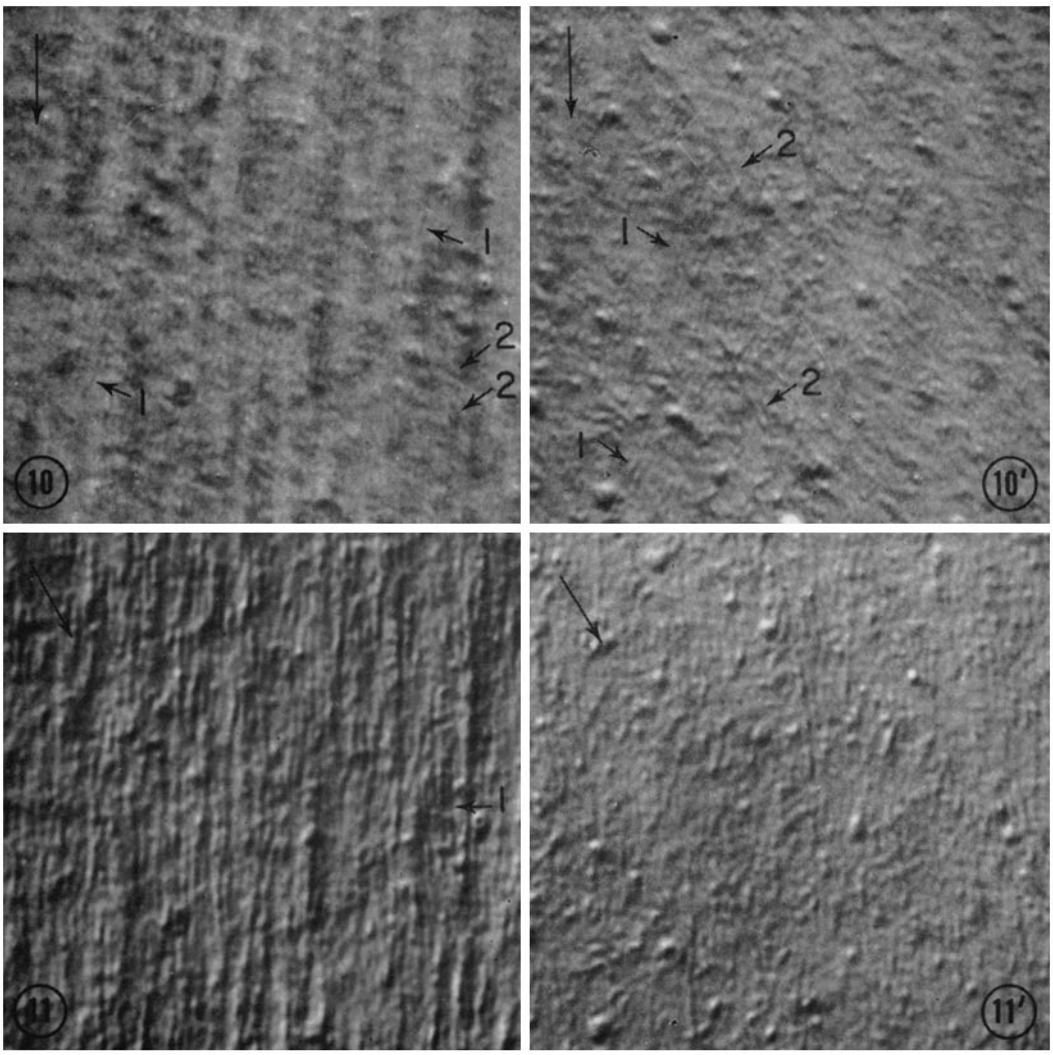

FIGURES 10–13 Longitudinal 2-μ Vestopal section stained with methylene blue. Differential interference 100/1.25. In each figure, the identical focal plane in the same area of the ectoplasm is depicted. The longitudinal axis of the axon is vertical. The series represents steps in one rotation experiment. Thus, as presented here, the direction of shear rotates in an anticlockwise manner as indicated by the large arrows.

FIGURE 10 Direction of shear parallel to long axis. Granular detail predominates. However, in two areas (arrows *1*) oblique strands run from NE to SW. Arrows *2* indicate short strands running obliquely in the opposite direction. × 3,000. FIGURE 11 Direction of shear oriented at 30° to the long axis. Long strands are contrasted running parallel to long axis. Arrow *1* indicates three strands with center-to-center spacing of 0.33 μ. × 3,000.

FIGURE 12 Direction of shear oriented at 50° to the long axis. The same longitudinal strands contrasted in Fig. 11 are depicted here (arrow *1*). In addition, strands run obliquely from NW to SE in two areas (arrows *2*). × 3,000. FIGURE 13 Direction of shear oriented at 90° to the long axis. The coarse, longitudinal elements represent unresolved groups of strands and associated granules (see Figs. 11 and 12). Small arrow indicates smallest center-to-center distance of 0.45 μ at this orientation. × 3,000.

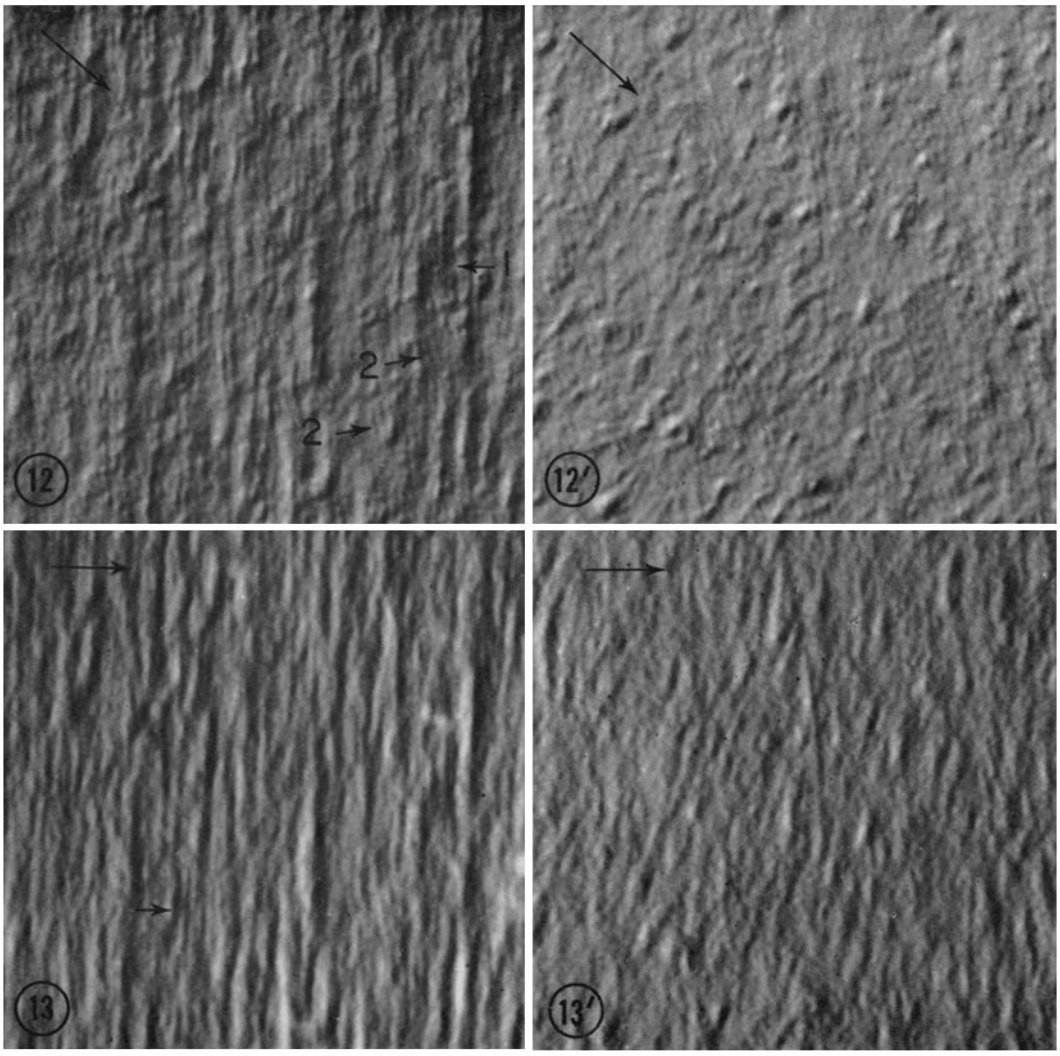

FIGURES 10′–13′ Longitudinal 2-μ Vestopal section stained with methylene blue. Differential interference 100/1.25. In each figure, the same area of the endoplasm is depicted and the level of focus identical. The longitudinal axis of the axon is vertical. The series represents steps in one rotation experiment. Thus, as presented here, the direction of shear rotates in an anticlockwise manner as indicated by the large arrows.

FIGURE 10′ Direction of shear oriented parallel to the long axis of the axon. Strands are oriented in a cross-lattice pattern: those running from NE to SW form prominent parallel arrays (arrows *1*); those running from NW to SE occur as single strands (arrows *2*). × 3,000. FIGURE 11′ Direction of shear oriented at 30° to the long axis of the axon. Short lengths of strands are oriented predominantly parallel to the long axis of the axon. Very few close groupings of strands are detectable. × 3,000.

FIGURE 12′ Direction of shear oriented at 50° to the long axis of the axon. In areas of the figure, parallel strands run at an angle of 20° to the long axis. × 3,000. FIGURE 13′ Direction of shear oriented at 90° to the long axis. Fine resolution is lacking at this orientation. The resolved thick elements run approximately parallel to the long axis of the axon.

length but branches and joins with other threads to form a complex three-dimensional network. Thus, the threads in the initial cross-lattice and those selectively resolved at each step in the rotation represent but fragments of the total network.

It was impossible to examine the fresh endoplasm with the 100/1.25 objective because of the short working distance of that lens. Analysis at this level of resolution is based solely upon sectioned material. However, the close structural correlation between the fresh and sectioned materials at lower levels of resolution indicates that the fixed material is truly representative of the fresh. Selected steps from a rotation series are illustrated in Figs. 10′–13′. The same area of the section is presented in each figure, and, as in the ectoplasmic series, the longitudinal axis of the axon is arranged vertically on the page. Hence, the direction of shear rotates in an anticlockwise direction from the long axis.

When the long axis of the axon is oriented parallel to the direction of shear (Fig. 10′), strands oriented in a cross-lattice pattern are contrasted. The angle between the two components of the lattice is the same as that observed in the fresh material at lower resolution, and the two components similarly lie symmetrically on either side of the direction of shear (compare Fig. 10′ with Figs. 5 and 14). The complexity of the cross-lattice, resolved as 0.33-μ strands, is illustrated to greater advantage in Fig. 17. Closely parallel strands occur in some areas (top left), and in others (arrow) individual strands interweave with one another in the depth of the optical section. In addition, short segments run at angles that are considerably larger, relative to the long axis of the axon, than those suggested by lower resolution micrographs.

On rotating the preparation, strands are selectively resolved at progressively smaller angles relative to the long axis of the axon. After 30° rotation, the selected strands lie parallel to the long axis of the axon (Fig. 11′). At this rotation step, the center-to-center spacing of the strands (0.33 μ) is the same as in the ectoplasm (Fig. 11), but the strands are shorter and the close groupings, seen in the ectoplasm, are less apparent. After 50° rotation (Fig. 12′), the closely spaced strands are oriented again at an angle of 20° to the longitudinal axis, and hence at 30° to the direction of shear. The larger granules, seen clearly in Figs. 10′ and 11′, are no longer sharply resolved from adjacent material. Fine resolution is largely lacking after 90° rotation (Fig. 13′), since the majority of the component strands of the space-network lie at angles of 60–90° relative to the direction of shear. The image structure, as in the ectoplasm, differs considerably from that at other orientations, but shows a predominantly longitudinal orientation of the extended thick elements. Important components of the thick elements in Fig. 13′ are the large granules, resolved in Figs. 10′ and 11′, but not resolved from adjacent material here.

THE SPACE-NETWORK OF THE ECTOPLASM AND ENDOPLASM: A SUMMARY Since the analysis of the fresh axoplasm was, of necessity, made with the differential interference microscope, the correlation between the structure of fresh and fixed axoplasm, and the extension of the analysis in fixed material, were also conducted by differential interference microscopy. Special features of the instrument (such as the directionality of the shadow-cast image and the selective resolution of fibrous material at particular orientations), and the problems introduced by these features into the interpretation of the spatial structure, determined that the one method be used throughout the analysis.

However, the conclusions drawn from the more elaborate analytical procedure described above, are portrayed clearly, and in synthesis, in Figs. 18 and 19. These micrographs were taken from unstained sections with 100/1.25 anoptral phase-contrast (Reichert). Fig. 18, illustrating the ectoplasm, shows the over-all parallel arrangement of 1.5–3.0-μ threads which branch and interconnect, and are resolved in some areas into 0.5-μ threads and in others into 0.3-μ strands. The strands branch at their own level of organization (arrow *1*), interweave in the close groupings, and cross from one grouping to another.

In contrast, the endoplasm (Fig. 19) lacks the parallel longitudinal orientation of its elements at each level of organization. The strands are oriented at many angles, but clearly form close groupings which also show a wide spread of angular orientation. Individual strands interconnect groupings (arrow *1*), and a few run almost at right angles to the long axis.

Electron Microscopy

Structural units of the same dimensions, form, angular orientations, and patterns of association as those described in fresh fibers can be discerned in survey electron micrographs from transverse and

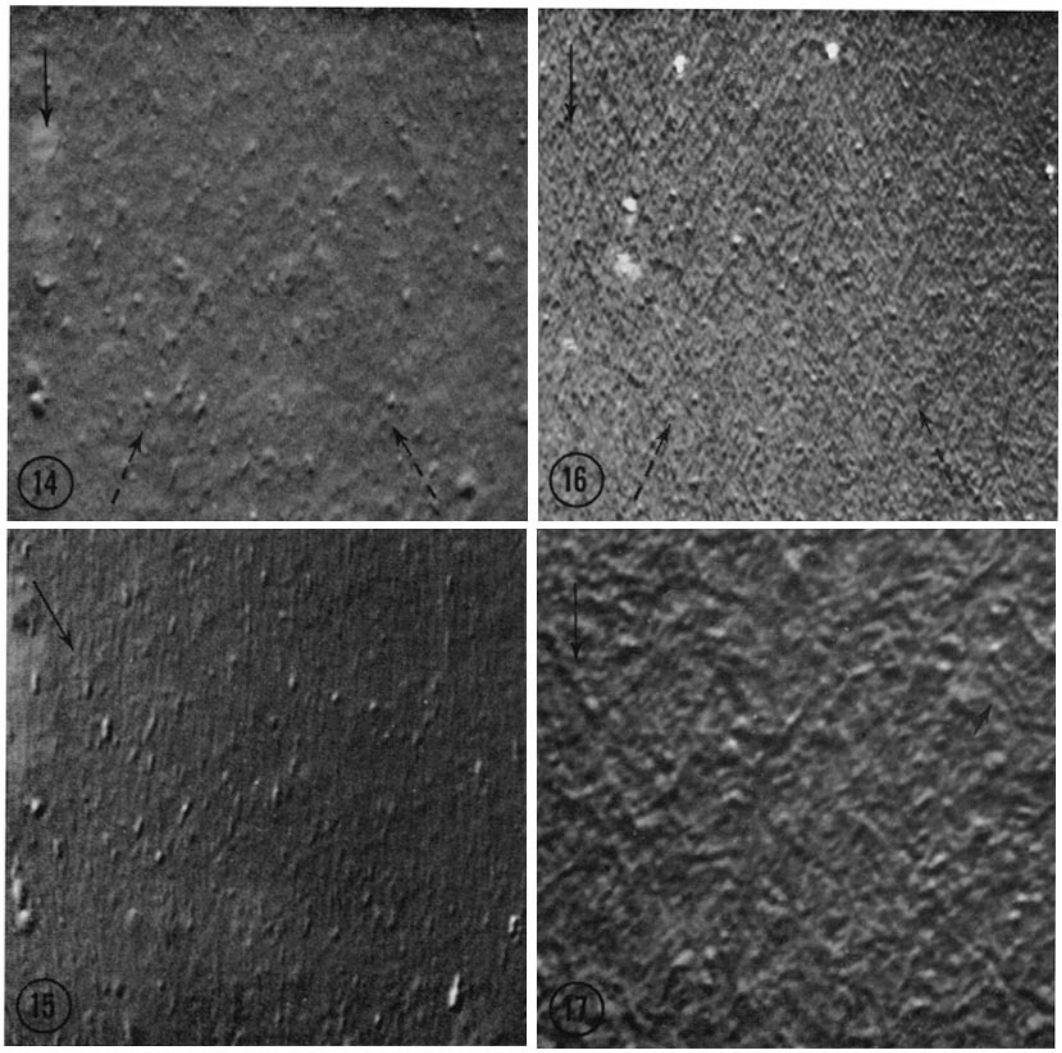

FIGURES 14 and 15 Optical sections of the endoplasm of the fresh giant nerve fiber. In both figures, the same area is depicted, the long axis of the axon is oriented vertical and the focal plane is almost identical (see large granules in each figure). Differential interference 40/0.85 oil. FIGURE 14 The long axis of the axon is oriented parallel to the direction of shear. A cross-lattice pattern, oriented symmetrically about the long axis of the axon, consists of rows of granules and very low-contrast threads. The broken arrows indicate the axes of the cross-lattice. × 1,200. FIGURE 15 The long axis of the axon is oriented at 30° to the direction of shear. Short threadlike elements run parallel to the long axis of the axon. × 1,200.

FIGURE 16 Longitudinal 2-μ Vestopal section of the endoplasm stained with methylene blue. Differential interference contrast 40/0.85 oil. The long axis of the axon is vertical and oriented parallel to the direction of shear. Cross-lattice pattern is prominent and consists of clearly resolved fibers. The angular spread of the cross-lattice is more or less identical to that in the fresh endoplasm (see Fig. 14). × 1,200.

FIGURE 17 Longitudinal unstained 2-μ Vestopal section of the endoplasm. Differential interference 100/1.25. The long axis of the axon is vertical and oriented parallel to the direction of shear. The cross-lattice is shown here as a complex system of strands. The predominant orientations are the same as those in Fig. 16. Individual strands run through the section at many other angles. The small arrow indicates a point at which strands are interwoven. × 3,000.

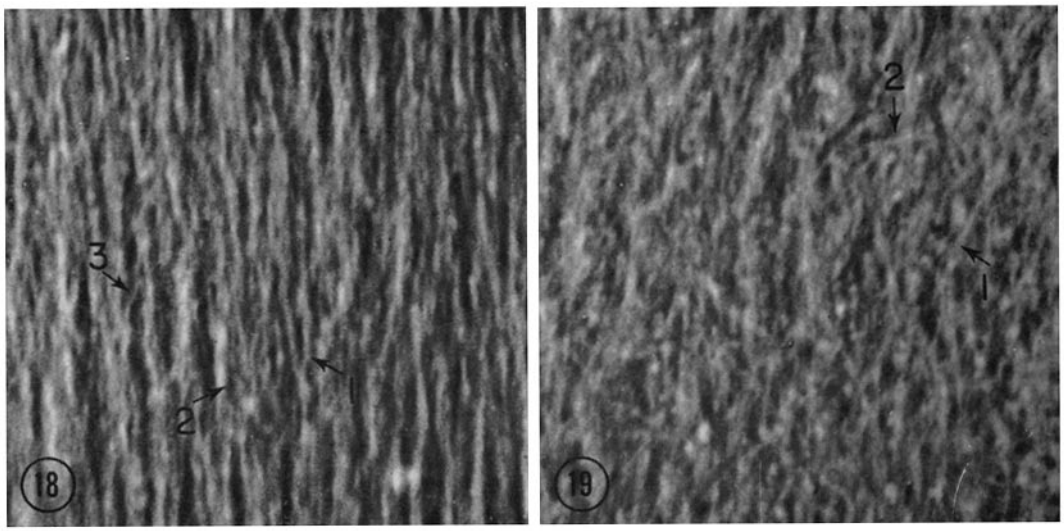

FIGURES 18 and 19 Longitudinal 2-μ unstained Vestopal sections of the giant nerve fiber. Reichert anoptral phase 100/1.25. The long axis is vertical in each figure. FIGURE 18 Area of the ectoplasm showing individual threads composed of 0.2–0.3-μ strands. The strands branch (arrow *1*), interweave (arrow *2*), and run from thread to thread (arrow *3*). × 2,250. FIGURE 19 Area of the endoplasm which lacks the predominantly longitudinal orientation of threads and strands. Arrow *1*, strand interconnecting threads. Arrow *2*, strands running almost transverse to the long axis. × 2,250.

longitudinal sections of the axoplasm. (Part of the results and conclusions of the electron microscopy of the squid giant nerve fiber is presented in another paper: see Metuzals, 1969.)

In the electron micrographs it is evident that the threadlike entities, as described so far in this investigation, must be considered as only parts of a continuous formation.

In survey electron micrographs of transverse sections of the axon, besides the profiles of mitochondria, the main structural components of the axoplasm appear as numerous small dots and short beaded threads (Fig. 20). These profiles measure 100–200 A in diameter and correspond to the *unit-filament strands* analyzed in detail in the following paper of Metuzals (1969), and to the neurofilaments of previous literature. The profiles of the unit-filament strands are distributed unevenly throughout the axoplasm, giving the cross-sectioned axoplasm a characteristic spotted pattern. Individual groups of densely packed profiles measure 0.1–0.3 μ in diameter and correspond to the smallest threadlike elements recognized by light microscopy in fresh and fixed preparations, namely the 0.35 μ strands. Areas in which the groups of profiles are themselves more closely spaced can be outlined. These areas range between 1 and 3 μ in diameter and correspond to the threads resolved in low-resolution light micrographs. However, a certain arbitrariness cannot be avoided in this delineation.

In survey electron micrographs from longitudi-

FIGURE 20 Survey electron micrograph of a transverse section through the giant nerve fiber. Note the profiles of the unit-filament strands appearing as small dots and short beaded lines. The density of their packing is greater towards the outer surface of the axon. The profiles are aggregated in 0.1–0.3-μ-wide strands (*S*). The boundary of a $\sim$ 2-μ-wide thread (*T*) is indicated by interrupted lines. Mitochondria (*M*); Schwann cells (*SW*); and connective tissue layers of the sheath (*C*). Fixed osmium tetroxide; stained uranyl acetate. × 27,000.

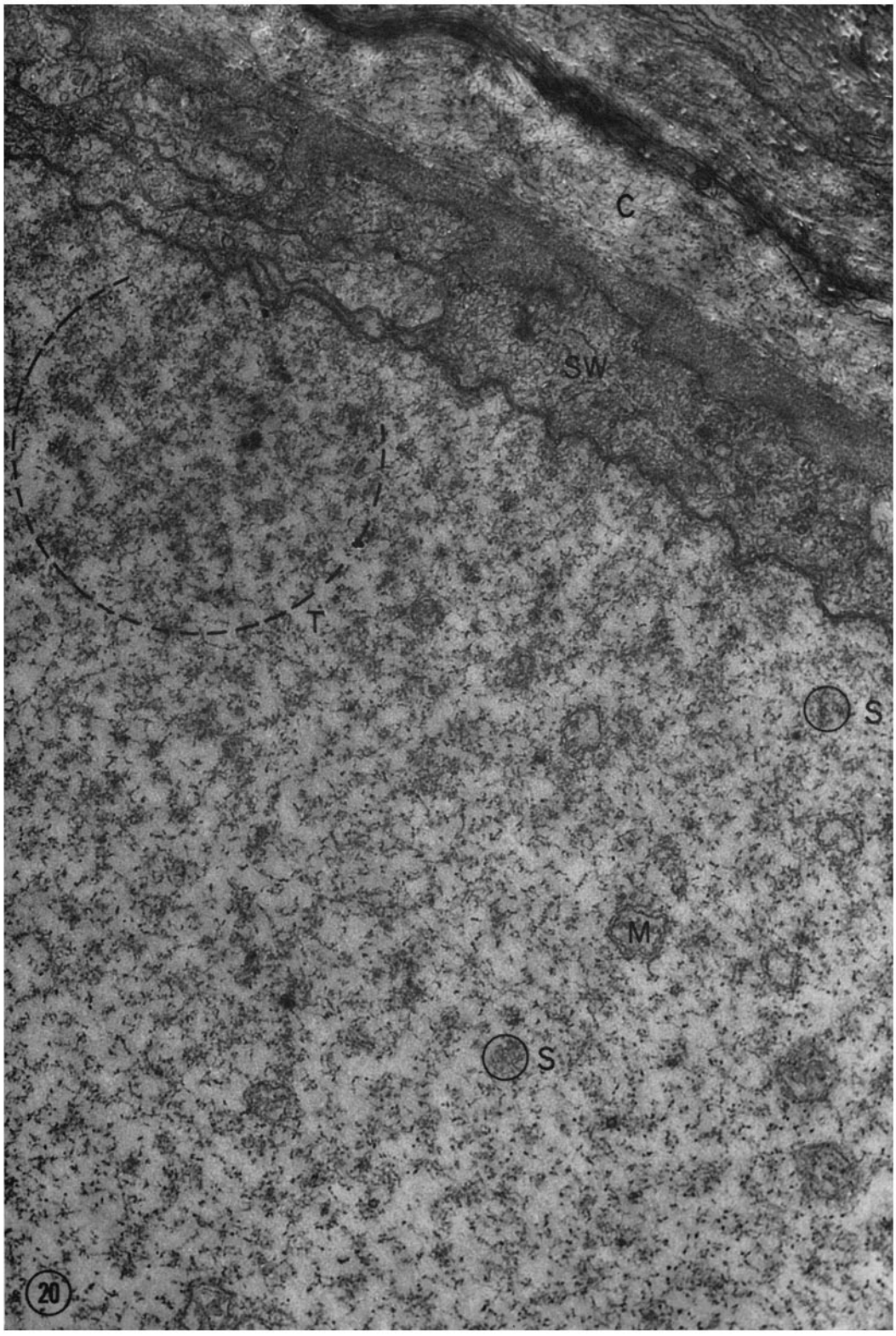
C
SW
T
S
M
S
20

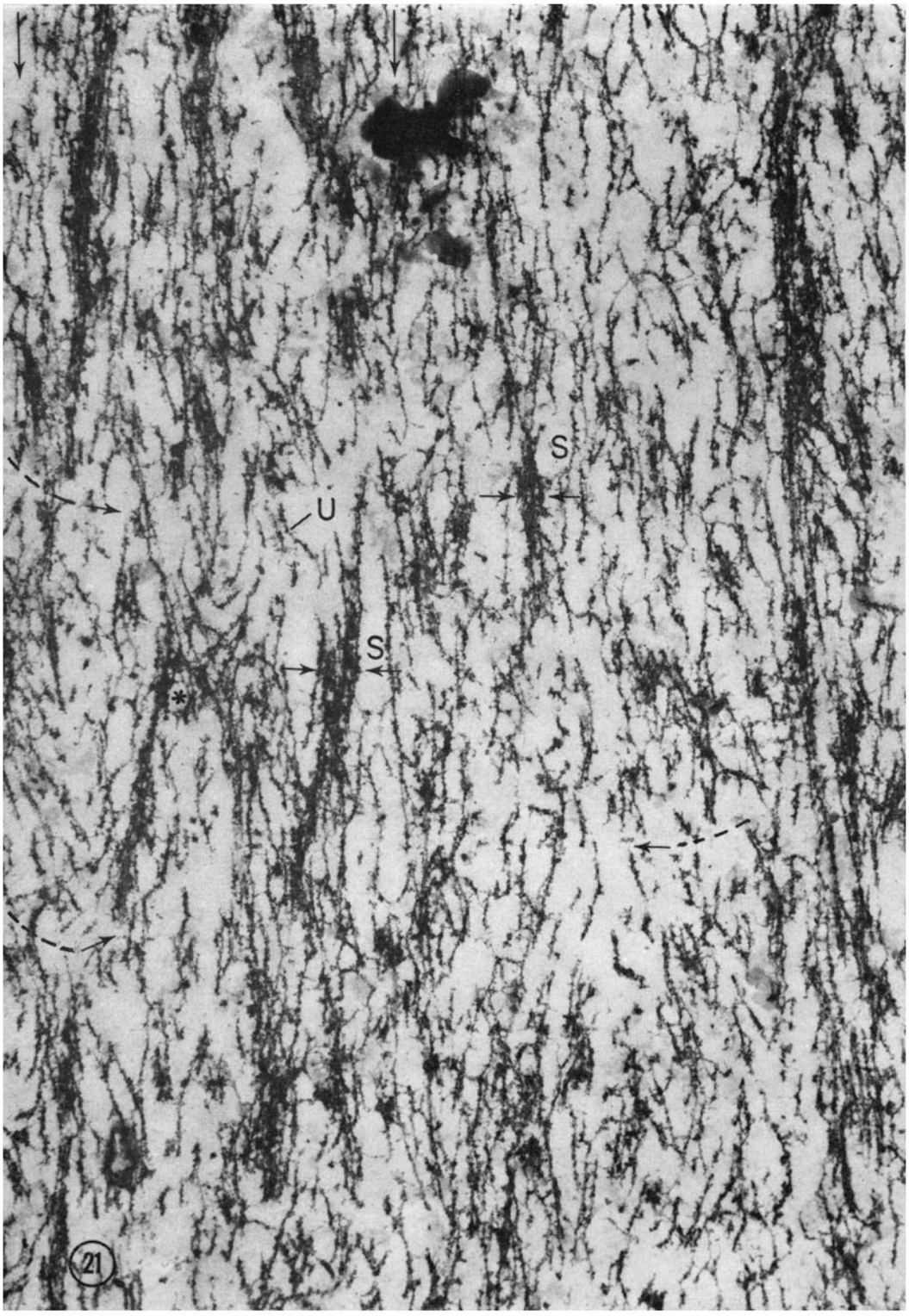

FIGURE 21 Survey electron micrograph of a longitudinal section through the axoplasm of the squid giant nerve fiber. The section is located in the middle part of the ectoplasm. The vertical arrows at the upper margin indicate the boundaries of a 3-μ-wide strand. 0.1–0.3-μ-wide strands (*S*); unit-filament strand (*U*). Interrupted arrows and the asterisk (see text). Fixed glutaraldehyde/osmium tetroxide; stained uranyl acetate and lead citrate. × 20,000.

nal sections, 0.1–0.3-μ strands often have a curved or sinuous appearance (*S*, Fig. 21). These strands do not extend longitudinally as uninterrupted elements throughout the micrograph. In narrow zones extending across the micrograph, the strands are interrupted by segments having a relatively less dense structural packing. The zones can be oriented perpendicular or oblique to the main direction of the strands, as indicated by the broken arrows in Fig. 21. Regularly, the orientation of the 0.1–0.3-μ strands reverses in adjacent densely packed segments separated by the zones mentioned above. This arrangement can be explained reasonably by assuming that the strands are helical. Helical strands having an amplitude greater than the section-thickness cannot appear in thin sections as continuous elements over long distances.

The 0.1–0.3-μ strands are composed of a number of interwoven unit-filament strands (*U*, Figs. 21 and 22). The latter are often interwoven around microtubules (*M*, Fig. 22), which represent another component of the strands. At sites within the micrograph, pairs of 0.1–0.3-μ strands approach and their component unit-filament strands intermingle to form a true branching-point (asterisk, Fig. 21). The regular occurrence of this feature in many survey micrographs demonstrates that the 0.1–0.3-μ strands branch and interconnect to form a continuous network.

The boundaries of a 2.5-μ-wide thread are indicated by the two vertical arrows at the upper margin of Fig. 21.

The unit-filament strands measure 70–250 A in diameter in electron micrographs taken at higher magnification (*U*, Fig. 22). They have a beaded appearance and frequently exhibit an irregular wavy course. Particularly the higher magnification electron micrographs demonstrate that unit-filament strands also do not extend as independent entities but are interwoven with other unit-filament strands.

In electron micrographs of the ectoplasm, the 1–3-μ-wide threads and the 0.1–0.3-μ-wide strands can be delineated more easily than in micrographs of the endoplasm. The arrangement of these threadlike elements is considerably looser in the endoplasm than in the ectoplasm. Often, a reticular array of the unit-filament strands predominates in the endoplasm without any preferred direction of orientation. In this reticulum single microtubules occur only rarely, whereas they are densely packed in the ectoplasm (see Metuzals, 1969). In survey electron micrographs, it is evident that no sharp boundary exists between ecto- and endoplasm.

DISCUSSION

Before we discuss the significance of the structural patterns observed in the axoplasm of the giant nerve fiber, it is necessary to consider to what extent these patterns represent the in vivo state. Intact, *in situ* nerve fibers and fresh preparations of isolated segments of fibers have the same structure at low magnification. Therefore, the isolation procedure does not appear to change significantly the structural pattern. Fresh preparations of segments of fibers retain the same structural pattern of threadlike elements for 1½ hr—the maximum period of use of such preparations—but after this period undergo organizational changes in the form of vesiculation of the peripheral axoplasm. That the fibrous structure of the axoplasm does not change during the period of observation is supported by the work of Bear et al. (1937 *b*). Their fresh preparations were dissected free for 6–7 cm, ligated at both ends, cut beyond the ties, and maintained in seawater. These preparations showed the same degree of birefringence as intact, undissected fibers still attached to the mantle muscles, and only after 1½ hr of isolation did the birefringence decrease and then rapidly. Our fresh preparations were transected only at their distal ends and thus maintained their connections with the cell bodies in the stellate ganglion.

The axoplasmic structures identified in the living axoplasm, and in fresh preparations, correlate very well with the structures observed in electron micrographs of fixed fibers. This supports the thesis that the structures have not changed significantly during preparation and observation and that they represent closely the living state.

The arrangement of the threadlike elements in a space-network accounts for the relative weakness of the birefringence of fresh axoplasm. According to Bear et al. (1937 *b*), this birefringence is only 3% of that of the A band in muscle. One would expect a higher degree of birefringence from the predominantly longitudinal orientation of the threads in low-resolution light micrographs. However, the further resolution of the threads into finer structures oriented over a wide range of angles accounts for the low-form birefringence of the axoplasm (Figs. 18 and 19). Conformational

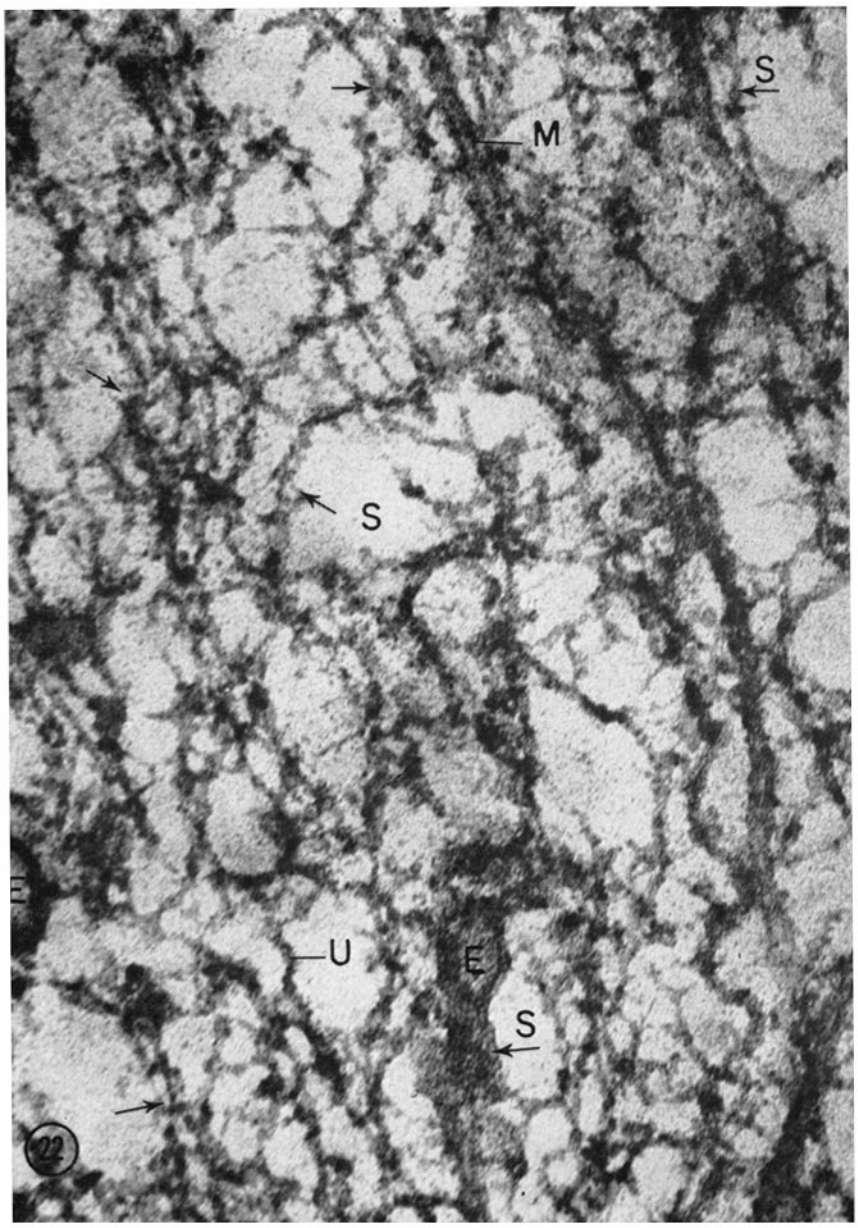

FIGURE 22 Electron micrograph of a longitudinal section through the ectoplasm of the squid giant nerve fiber. Unit-filament strands (*U*) are interwoven with each other and with microtubules (*M*) in a continuous network formation. However, boundaries of 0.1–0.3-μ-wide strands (*S*) can be identified and are indicated in the figure by opposed arrows. Profiles of the smooth endoplasmic reticulum (*E*). Fixed PTA/glutaraldehyde/osmium tetroxide; stained uranyl acetate and lead citrate. × 140,000.

changes in certain components of such a continuous space-network would not affect greatly the form birefringence of the whole axoplasm. Expressed as changes in birefringence, such conformational changes may appear small or be undetectable.

During the rotation of the endoplasm, the selection of threads by the differential interference

microscope over a continuous range of angles between the two components of the initial cross-lattice may give the impression that, within these limits, the orientation of the threads is more or less random, i.e. that the network has little definable regularity. This is not the case; regularity exists at each level of the structural hierarchy. Thus, the unit-filament strand, the strand, and the thread, have each a definable form and size and, although lying at all angles between the cross-lattice, are nevertheless spaced in a definable way relative to one another. Through this regularity the differential interference microscope selects fragments of the network that, at any angle, appear as threadlike elements extending uninterrupted, and often as discrete units, through considerable distances of what we know to be a fine network.

A number of experiments support our observation of the existence of a peripheral, denser ectoplasmic region and a central core of a less dense endoplasm. Thus, Chambers (1947), and Chambers and Kao (1952) inferred from the microinjection of oil drops and dyes a longitudinal ultrastructure throughout the axoplasm, the density of which decreases on passing from the periphery to the center of the axon. Chambers and Kao (1952) accounted for the different widths of the ovoid oil drops only in terms of a greater density of the longitudinal ultrastructure in the peripheral axoplasm. However, although our structural observations demonstrate that there is a greater density of fibrous material in the periphery than in the center of the axon, the more parallel arrangement of this fibrous material in the ectoplasm can equally account for their observed differences in the shape of the drops.

In addition, Baker et al. (1962) stated that in perfused fibers the axon membrane appears to be protected by a thin, robust film of axoplasm. Bear et al. (1937 *a*) could distinguish a thin membrane surrounding the extruded axoplasmic rod. It appeared to be part of the axoplasm and not of the Schwann sheath. Occasionally, these authors observed that the central axoplasmic material could flow out from this membrane. A new film was not formed and the old membrane trailed behind the central axoplasmic material. Again, these observations conform with our view of a structurally more dense ectoplasm.

The space-network with its structural hierarchy of intercoiled threadlike elements is a configuration that can be considered primarily responsible for the gel-state properties of the axoplasm (see Ferry, 1948). The highly ordered structure of the space-network ranges from the level of aggregates of protein macromolecules up to the level of light microscopic arrays, and culminates in the ecto- and endoplasmic differentiation and the large-scale helical configuration within the axon. The space-network is a configuration that would also permit graded and reversible changes in the gel-state properties of the axoplasm and may be associated causally with axonal streaming processes. Coiling/decoiling and folding/unfolding of the threadlike elements, combined with a sliding of the elements over one another, could represent the primary mechanisms in such processes (see Metuzals, 1969). The differentiation of the axon into the more solid ectoplasm and the less solid endoplasm can be considered from this viewpoint (see also Goldacre and Lorch, 1950; Poglazov, 1966).

It is worthwhile to speculate about the significance of the ecto- and endoplasmic differentiation and about the transformation in more detail. Through decoiling and unfolding, the threadlike elements would straighten out and become oriented more parallel. At the same time, their increased density would allow a greater number of sites of contact. This could account for the greater stability, or more solid character, of the ectoplasm. Conversely, coiling and folding of the threadlike elements would decrease their parallel arrangement and the number of contact sites (see Ferry, 1948). This looser array could account for the less solid character of the endoplasm. That changes between the ecto- and endoplasmic configurations occur, is indicated by the considerable variations in the structure of the endoplasm along the fiber axis, as described on page 460.

Furthermore, the observed differences in the structural configurations of the ectoplasm and the endoplasm could be responsible for the maintenance of and lability of diffusion barriers and hence possibly slight potential differences in the axoplasm (see also Goldacre, 1952; Ling, 1960).

There is no doubt that calcium ions influence strongly the gel-state properties of the axoplasm. For example, calcium injected into the squid giant axon by means of a microsyringe causes liquefaction of the axoplasm (Chambers and Kao, 1952). In addition, the injection changes the membrane potential and tends to block impulse conduction. According to Hodgkin and Keynes (1956), it seems likely that these effects of calcium are a gen-

eral consequence of disrupting the internal structure of the axon, rather than a special action on the membrane itself, although the bulk of neurophysiological evidence indicates that conduction is a pure membrane phenomenon. In this context, it should be mentioned that the nervous impulse is accompanied by changes in light-scattering properties of the axoplasm of the squid giant nerve fiber; the scattering originates from at least two phenomena (Cohen et al., 1968). The failure of the light scattering to return to the original intensity after 10 msec suggests the occurrence of some long-lasting structural changes. These observations indicate that a full knowledge of the structure of the living axoplasm is essential for a complete understanding of the many different functional aspects of the neuron—such as metabolism, axonal streaming, synaptic transmission, as well as ceraint aspects of impulse conduction.

The authors gratefully acknowledge the generous support for this work given by the Medical Research Council of Canada in a grant (MA-1247) to one of us (Dr. Metuzals) and the support given to the other author (Dr. Izzard) by the National Institute of General Medical Science through the Program-Project grant (G 19-14891-02) administered by Dr. R. D. Allen.

Special thanks are given to the chairman of the Medical Research Council of Canada, Dr. G. Malcolm Brown, for his understanding in allocating funds for the work at Woods Hole and to Dr. R. D. Allen, State University of New York at Albany for his encouragement and helpful advice with reference to the light microscopy.

The helpful support by Carl Zeiss, Inc. (Dr. E. Bieber) during their exhibition in Woods Hole, summer 1968, is acknowledged.

Excellent assistance during all phases of this investigation has been given by the following persons: Mr. M. Gospodnetić, medical student at the University of Ottawa; Mrs. P. Borysowich (electron microscopy); and Mr. G. Chantigny (photography).

Received for publication 20 March 1969, and in revised form 29 July 1969.

REFERENCES

ALLEN, R. D., G. B. DAVID, and G. NOMARSKI. 1969. *Z. Wiss. Mikrosk.* In press.

BAJER, A., and R. D. ALLEN. 1966 *a*. Structure and organization of the living mitotic spindle of Haemanthus endosperm. *Science.* **151**:572.

BAJER, A., and R. D. ALLEN. 1966 *b*. Role of the phragmoplast filaments in cell-plate formation. *J. Cell Sci.* **1**:455.

BAKER, P. F., A. L. HODGKIN, and T. I. Shaw. 1962. Replacement of the axoplasm of giant nerve fibers with artificial solutions. *J. Physiol.* **164**:330.

BEAR, R. S., F. O. SCHMITT, and J. Z. YOUNG. 1937 *a*. Investigations in the protein constituents of nerve axoplasm. *Proc. Roy. Soc. Ser. B.* **123**:520.

BEAR, R. S., F. O. SCHMITT, and J. Z. YOUNG. 1937 *b*. The ultrastructure of nerve axoplasm. *Proc. Roy. Soc. Ser. B.* **123**:505.

CHAMBERS, R. 1947. The shape of oil drops injected into the axoplasm of the giant nerve of the squid. *Biol. Bull.* **93**:191.

CHAMBERS, R., and C. Y. KAO. 1952. The effect of electrolytes on the physical state of the nerve axon of the squid and of stentor, a protozoon. *Exp. Cell Res.* **3**:564.

COHEN, L. B., R. D. KEYNES, and B. Hille. 1968. Light scattering and birefringence changes during nerve activity. *Nature.* **218**:438.

FERRY, J. D. 1948. Protein gels. *In* Advances in Protein Chemistry. M. L. Anson and J. T. Edsall, editors. Academic Press Inc., New York. 1–78.

FRANÇON, M. 1961. Progress in Microscopy. Row, Peterson Co., New York.

GEREN, B. B., and F. O. SCHMITT. 1954. The structure of the Schwann cell and its relation to the axon in certain invertebrate nerve fibers. *Proc. Nat. Acad. Sci. U.S.* **40**:863.

GOLDACRE, R. J. 1952. The folding and unfolding of protein molecules as a basis of osmotic work. International Review of Cytology. G. H. Bourne and J. F. Danielli, editors. Academic Press Inc., New York. **1**:135–164.

GOLDACRE, R. J., and I. J. LORCH. 1950. Folding and unfolding of protein molecules in relation to cytoplasmic streaming, amoeboid movement and osmotic work. *Nature.* **166**:497.

HODGKIN, A. L., and A. F. HUXLEY. 1945. Resting and action potentials in single nerve fibers. *J. Physiol.* **104**:176.

HODGKIN, A. L., and B. KATZ. 1949. The effect of calcium on the axoplasm of giant nerve fibers. *J. Exp. Biol.* **26**:292.

HODGKIN, A. L., and R. D. KEYNES. 1956. Experiments on the injection of substances into squid giant axons by means of a microsyringe. *J. Physiol.* **131**:592.

LING, G. N. 1960. The interpretation of selective ionic permeability and cellular potentials in terms of the fixed change-induction hypothesis. *J. Gen. Physiol.* **43**:149.

METUZALS, J., C. S. IZZARD, and M. GOSPODNETIĆ.

1968. Observations of living giant nerve fibers of the squid by differential interference-contrast microscopy. *Biol. Bull.* **135:**411.

METUZALS, J. 1969. Configuration of a filamentous network in the axoplasm of the squid (*Loligo pealii* L.) giant nerve fiber. *J. Cell Biol.***43:**480.

NOMARSKI, G. 1955. Microinterférométrie différentielle à ondes polarisées. *J. Phys. Radium.* **16:**9s.

PADAWER, J. 1968. The Nomarski interference-contrast microscopy. An experimental basis for image interpretation. *J. Roy. Microsc. Soc.* **88:**305.

POGLAZOV, B. F. 1966. Structure and Functions of Contractile Proteins. Academic Press Inc., New York, London.

RICHARDSON, K. C., L. JARETT, AND E. H. FINKE. 1960. Embedding in epoxy resins for ultrathin sectioning in electron microscopy. *Stain Technol.* **35:** 313.

SCHMITT, F. O., and B. B. GEREN. 1950. The fibrous structure of the nerve axon in relation to the localization of "neurotubules." *J. Exp. Med.* **91:**499.

VILLEGAS, G. M., and R. VILLEGAS. 1960 *a*. The ultrastructure of the giant nerve fiber of the squid: Axon-Schwann cell relationship. *J. Ultrastruct. Res.* **3:**362.

VILLEGAS, R., and G. M. VILLEGAS. 1960 *b*. Characterization of the membranes in the giant nerve fiber of the squid. *J. Gen. Physiol.* **43:**73.

YOUNG, J. Z. 1937. The structure of nerve fibers in cephalopods and crustacea. *Proc. Roy. Soc. Ser. B.* **121:**319.